University of Hertfordshire UH 25

Research Archive

Citation for published version:

J. C. Beamin, et al, 'Searching for faint comoving companions to the α Centauri system in the VVV survey infrared images', *Monthly Notices of the Royal Astronomical Society*, Vol. 472 (4): 3952-3958, December 2017.

DOI:

https://doi.org/10.1093/mnras/stx2144

Document Version:

This is the Published Version.

Copyright and Reuse:

© 2017 Crown Copyright.

Content in the UH Research Archive is made available for personal research, educational, and non-commercial purposes only. Unless otherwise stated, all content is protected by copyright, and in the absence of an open license, permissions for further re-use should be sought from the publisher, the author, or other copyright holder.

Enquiries

If you believe this document infringes copyright, please contact the Research & Scholarly Communications Team at rsc@herts.ac.uk

Searching for faint comoving companions to the α Centauri system in the VVV survey infrared images

J. C. Beamín,[1,2★] D. Minniti,[2,3,4] J. B. Pullen,[3] V. D. Ivanov,[5,6] E. Bendek,[7] A. Bayo,[1] M. Gromadzki,[8] R. Kurtev,[1,2] P. W. Lucas[9] and R. P. Butler[10]

[1]*Instituto de Física y Astronomía, Facultad de Ciencias, Universidad de Valparaíso, Ave. Gran Bretaña 1111, Playa Ancha, Valparaíso 2360102, Chile*
[2]*Millennium Institute of Astrophysics, Astronomy Department, University of Chile, Mario Hamuy 7500011, Chile*
[3]*Facultad de Ciencias Exactas, Universidad Andres Bello, Fernandez Concha 700, Las Condes, Santiago 7591538, Chile*
[4]*Vatican Observatory, I-V00120 Vatican City State, Italy*
[5]*European Southern Observatory, Karl-Schwarzschild-Str. 2, D-85748 Garching bei München, Germany*
[6]*NASA Ames Research Center, Moffett Field, CA 94035, USA*
[7]*NASA AMES, CA, USA*
[8]*Warsaw University Astronomical Observatory, Al. Ujazdowskie 4, PL-00-478 Warszawa, Poland*
[9]*Centre for Astrophysics Research, University of Hertfordshire, Hatfield AL10 9AB, UK*
[10]*Department of Terrestrial Magnetism, Carnegie Institution of Washington, 5241 Broad Branch Road, NW, Washington, DC 20015-1305, USA*

ABSTRACT

The VVV survey has observed the southern disc of the Milky Way in the near-infrared, covering 240 deg^2 in the *ZYJHK*$_s$ filters. We search the VVV survey images in a ∼19 deg^2 field around α Centauri, the nearest stellar system to the Sun, to look for possible overlooked companions that the baseline in time of VVV would be able to uncover. The photometric depth of our search reaches $Y \sim 19.3$ mag, $J \sim 19$ mag, and $K_s \sim 17$ mag. This search has yielded no new companions in α Centauri system, setting an upper mass limit for any unseen companion well into the brown dwarf/planetary mass regime. The apparent magnitude limits were turned into effective temperature limits, and the presence of companion objects with effective temperatures warmer than 325 K can be ruled out using different state-of-the-art atmospheric models. These limits were transformed into mass limits using evolutionary models, companions with masses above 11M$_{Jup}$ were discarded, extending the constraints recently provided in the literature up to projected distances of $d < 7000$ au from α Cen AB and ∼1 200 au from Proxima. In the next few years, the VVV extended survey (VVVX) will allow us to extend the search and place similar limits on brown dwarfs/planetary companions to α Cen AB for separations up to 20 000 au.

Key words: brown dwarfs – planetary systems – infrared: planetary systems.

1 INTRODUCTION

The nearest stellar system α Centauri (including the close binary α Cen AB and Proxima) allows us to probe to unprecedented depth the vicinity of three stars for planets. α Cen AB is three times closer than any other FGK star offering unique conditions for detection and characterization of Earth-like planets around Sun-like stars in terms of brightness and angular separation of a hypothetical habitable planet. However, the system has not been considered in the target list of exoplanet imaging missions because of light contamination of the environs of each binary component by the other. Recent advances in binary star light suppression and wavefront control (Thomas, Belikov & Bendek 2015) has enabled the creation of dark zones around binary systems. As a result, dedicated mission concepts to

observe α Centauri has been proposed (Bendek et al. 2015) with telescopes as small as 40 cm in aperture. Scientists and engineers (Sirbu, Thomas & Belikov 2017) are also studying whether the *WFIRST* coronagraph would be able to observe binaries and include α Cen in the target list.

It is worth mentioning that detecting an Earth-like planet in the habitable zone of α Cen AB with a 40-cm aperture telescope is equivalent, in terms of photon flux and angular separation, to performing the same detection around a star at 10 pc with a 4-m-class NASA's 'HABEX' flagship exoplanet mission.

This system will be an important target to be further explored with the next generation of space telescopes and missions and of the Breakthrough Starshot project.[1]

★ E-mail: juancarlos.beamin@ifa.uv.cl

[1] http://breakthroughinitiatives.org/Initiative/3

A planet on a 3.2 d orbit was reported to exist around α Cen B Dumusque et al. (2012), but more recent studies cast doubts on the existence of this planet, arguing that the signal reported by Dumusque et al. (2012) 'arise from the window function of the observed data' (Rajpaul, Aigrain & Roberts 2016). Demory et al. (2015) looked for evidence of α Cen Bb using *HST*/STIS photometry. They found no evidence of the proposed α Cen Bb, but, on the other hand, reported the presence of a transit-like feature in the light curve of α Cen B, that might be produced by an earth-mass planet in an ∼15–20 d orbit. Kervella et al. (2006) studied α Cen AB, with the NACO instrument at VLT, and set upper limits for a possible comoving companion in the *H* and *K* band, corresponding to ∼20–30 M_{Jup} with separations between 7 and 20 au. Later, Kervella & Thévenin (2007) using optical imaging (*V*, *R*, *I* and *Z* bands) complemented this search and determined that there were no comoving companions to this system with masses ≳ 15–30M_{Jup} at separations between 100–300 au

Quarles & Lissauer (2016) investigated numerically if stable planetary orbits exists around one of the stars or around the α Cen AB binary, and arrived at a positive answer (see their Fig. 11).

Recently, Pourbaix & Boffin (2016) and Kervella et al. (2016) performed a detailed astrometric study of the α Cen AB system, and derived not only precise proper motion (PM) and parallaxes, but also orbital parameters and in the latter case predictions of microlensing events in the following years, that would allow us to probe an unexplored parameter space for the presence of exoplanets around those stars.

Regarding Proxima: Benedict et al. (1999) found no companions with masses above 0.8 M_{Jup} in the period range $1 \leq P$ (d) ≤ 1000, using *HST* Guide Sensor data. Endl and Kürster (2008), based on nearly 7 yr of radial velocity measurements, found no evidence of planets with masses larger than $M \sin(i) \geq 1M_{Neptune}$, at periods ≤ 2.7 yr.

Lurie et al. (2014) using ground-based astrometric measurements constrained the presence of planets with masses down to 2M_{Jup} with periods $2 \leq P$ (yr) ≤ 5, and down to 1M_{Jup} for $5 \leq P$ (yr) ≤ 12. As pointed by Lurie et al. (2014), these studies eliminate the possibility of finding any Jupiter-like planet around Proxima for orbital periods out to 12 yr. Recently a rocky planet in an 11-d orbit was reported by Anglada-Escudé et al. (2016), making Proxima b the closest exoplanet known.

Mesa et al. (2017) searched for the presence of giant exoplanets around Proxima using high-contrast imaging with the SPHERE instrument at the Very Large Telescope: No objects were found with masses above 6–7 M_{Jup} at 0.5–1 au, and 4M_{Jup} at distances larger than 2.5 au, using the AMES-COND models (Baraffe et al. 2003).

We have investigated the presence of substellar companions with separations up to 7000 au from α Cen and up to 1 200 au from Proxima. This paper is organized as follows: Section 2 describes the observations, Section 3, the manual and automated search for faint companions. Section 4 is dedicated to the discussion of the limits imposed by our search, and the final Section 5 gives the conclusions.

2 SAMPLE SELECTION AND OBSERVATIONS

2.1 VISTA/VIRCAM

The VVV survey (Minniti et al. 2010; Saito et al. 2012; Hempel et al. 2014) was one of the six ESO public surveys carried out with the 4.1 m Visual and Infrared Survey Telescope for Astronomy (VISTA) telescope and VIRCAM camera (Dalton et al. 2006;
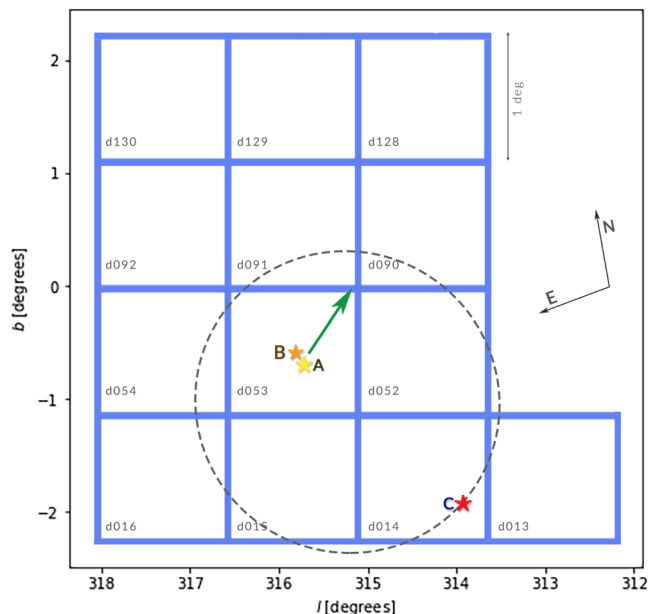

Figure 1. Field of view analysed in this study, each rectangle corresponds to one VVV tile. The position of the α Cen AB system is marked in yellow-orange (separation not to scale) stars and Proxima as a red star. The grey ellipse shows an approximate orbit of Proxima around the AB pair, from Kervella, Thévenin & Lovis (2017). The green arrow shows the PM of the system. The total area covered by this search is ∼19 deg². The limiting distance of 7000 au (and 1200 to Proxima) is given by the distance to the south-east limit of the tile 'd015' (and 'd014' for Proxima). To the north-east and north-west, the limiting separation almost reaches 20 000 au from α Cen AB.

Emerson & Sutherland 2010) at cerro Paranal Chile. The VIRCAM detector has sixteen chips of 2048 × 2048 pixels with a pixel scale of 0.34 arcsec . The total area covered after six overlapping pointings (known as 'pawprints') is $1 \times 1^{\circ}5$ (hereafter a 'tile'). VVV had a multicolour campaign in five near-infrared (NIR) bands (*ZYJHK*s) in the first year (2010), and then 5 yr of monitoring in the K_s band, where the total number of epochs differed from field to field from almost 300 epochs in some bulge fields to 54 epochs in the least observed disc field. Additionally, during the last year of the survey (2015) one/two extra epochs were obtained in the *ZYJH* bands. The main goal of VVV was to trace the 3-D structure of the Milky Way, mainly through the study of variable stars (Dékány et al. 2013) but also using red clump stars (Gonzalez et al. 2011) and NIR mutiwavelength studies (Minniti et al. 2014). This survey is useful for accurate measurements of PMs and parallaxes, as demonstrated previously by Beamín et al. (2013), Ivanov et al. (2013), Beamín et al. (2015), Smith et al. (2015), Kurtev et al. (2017), Beamin et al. (2017) and Smith et al. (2017). The data used in this study, were reduced at the Cambridge Astronomy Survey Unit (CASU) with PIPELINE v1.3. In this study, we considered 13 different tiles, two epochs in the *Y* and *J* bands and three epochs for the K_s band.

3 METHODS

3.1 Visual inspection of images

We created false colour images for 13 tiles using K_s images taken at three epochs separated in time by approximately 2 yr from each other. The total area covered by the images was ∼19 deg² (See Fig. 1). A source with the same motion of the α Cen system would
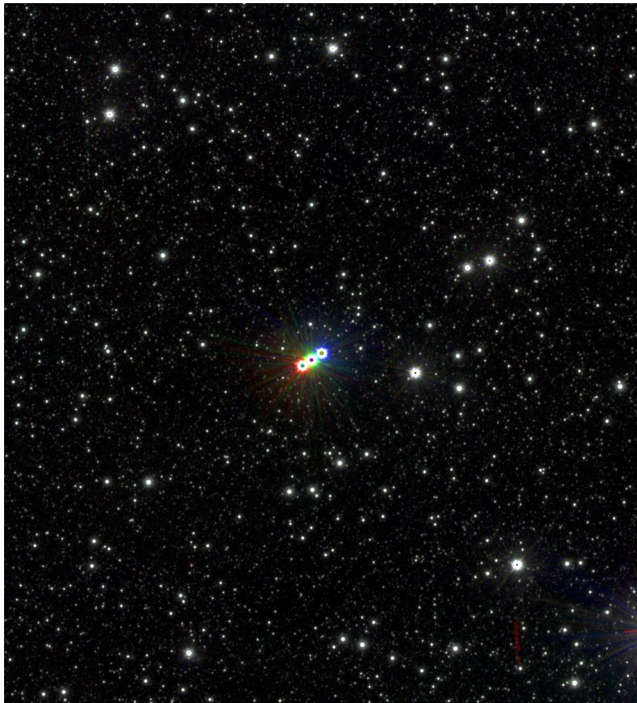
Figure 2. Colour composite image of Proxima. We used three K_s epochs: 2010, 2012 and 2014 colours are red green and blue, respectively. The motion is evident on the image at the bottom right-hand side. This image highlights the motion of the bright star Proxima, but additional colour enhancement was used to search for the faintest moving target across the images.

have left an easily recognizable colour trace with the same position angle as the PM of the α Cen system. All non-variable sources would appear white, variables of high amplitude would have a point-like shape and the colour skewed to the colour assigned to the epoch at maximum brightness. Very high PM sources like Solar system objects would be detected only in one image and be detected as a point-like source with only one colour. Other high PMs sources would appeared as elongated sources with red and blue colours at the edges (Fig. 2 shows this feature for Proxima). Other artefacts like ghosts, diffraction spikes, etc., would not produce a linear trace of point-like sources in any case, so it did not affect our visual search.

With this method, we can reject the presence of an extra component to the system down to $K_s \sim 17$–17.5 mag, which is the 5σ point source magnitude limit detection per epoch, and mainly discard sources around very bright and saturated stars.

3.2 Source catalogue cross matching

Following the visual inspection, we retrieved catalogues for 13 different pointings (tiles) from two epochs separated by $\sim$5 yr in the Y and J bands from the VVV survey. We choose to use the images in Y and J bands because these images are deeper than H and K_s and also more sensitive to ultra cool ($T_{\rm eff} \leq 500$ K) brown dwarfs (BD) in the NIR, than the K_s band (Beamín et al. 2014; Morley et al. 2014; Luhman & Esplin 2016; Schneider et al. 2016; Zapatero Osorio et al. 2016; Leggett et al. 2017). H band is also sensitive to UCDs, but in our survey is shallower than Y and J bands, so this would not improve the detectability of a UCD.

The total time span between the two Y and J band observations is 5 yr (2010–2015). Additionally, Y and J band epochs are usually

Table 1. 5σ limiting magnitude for the tiles analysed in this work.

| Tile name	Y_{2010} (mag)	Y_{2015} (mag)	J_{2010} (mag)	J_{2015} (mag)
d013	19.55	19.34	19.24	19.14
d014	19.50	19.30	18.71	19.05
d015	19.48	19.44	18.92	18.92
d016	19.44	19.41	18.77	19.03
d052	19.86	19.54	19.57	19.33
d053	19.97	19.61	19.29	19.17
d054	20.13	19.69	19.43	19.26
d090	20.01	19.72	19.53	19.4
d091	19.91	19.57	19.55	19.45
d092	19.60	19.56	19.36	19.28
d128	19.85	19.64	19.42	19.25
d129	19.62	19.51	19.41	19.39
d130	19.53	19.42	19.32	19.25
Adopted	19.3		19.	
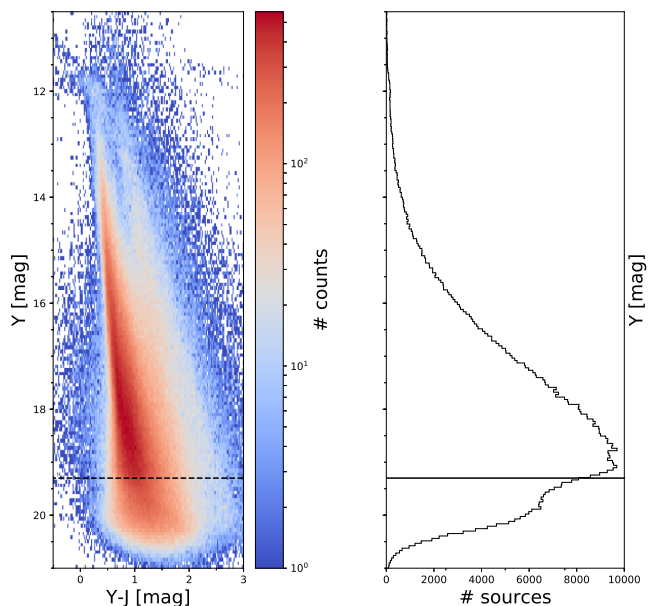
Figure 3. Left-hand panel: CMD of tile d053. Right-hand panel: histogram of sources in the Y band presented in the CMD.

not taken simultaneously. Images from the same year for the Y and J bands for 8 out of the 13 tiles were obtained with a time difference larger than 20 d at least in one epoch, 20 d is the required time for a source comoving with the α Cen system to move $\sim$0.6 pixels in the VIRCAM camera, and hence produce a shift in the centroid of 0.1 arcsec of the background source, assuming both sources have similar fluxes. This implies that we effectively had three or four epochs, decreasing significantly the already low chance of an alignment between a possible companion of α Cen system and a background source. The dates of each individual image in Y and J bands are given in Table A1 in the appendix.

The first epoch was observed usually between 2010 March and April, and the second epoch around 2015 May–June. For these catalogues, the 5σ limiting magnitudes are $Y \sim 19.3$ and $J \sim 19.0$ mag. A list of the values per tile is given in Table 1.

A typical colour–magnitude diagram (CMD) in the Y and J bands is shown in Fig. 3; in this case, we selected sources from tile d053 (containing α Cen), which is the least detection favouring tile due to the saturation, spikes and 'image ghosts'. Nevertheless, over

Table 2. Astrometry of α Cen system.

Star name	$\mu\alpha\cos\delta$ (mas yr^{-1})	$\mu\delta$ (mas yr^{-1})	π (mas)
α Cen A[a]	−3619.9	693.8	747.17
α Cen B[a]	−3619.9	693.8	747.17
α Cen C[b] (Próxima)	−3773.84	770.54	768.7

[a]Kervella et al. (2016); [b]Benedict et al. (1999).

700 000 sources were cross-matched between the two bands. Additionally, we included the histogram in *Y* magnitude and the 5σ photometric detection limit (*Y* = 19.3 mag) as a dashed line in the CMD and solid black line and in the histogram. The remaining 12 tiles analysed in this study share similar number counts and overall shape of the CMD, with a very strong disc sequence and a less populated sequence of giant stars to the right, typical for the inner region of the disc population and the expected colour spread due to interstellar extinction.

To search for comoving companions, we first performed a cross-match between the two epochs of the same band (*Y* and *J* bands, respectively), we used STILTS to perform the cross-match (Taylor 2005). A 0.7 arcsec tolerance radius (2 pixels) was defined for the match, and we kept only sources that do not have a counterpart in the other epoch, effectively removing the low PM sources.

To the remaining stars, we applied the PM and parallax motion corresponding to each member of the α Cen system separately (α Cen AB barycentric motion from Kervella et al. 2016 and Proxima from Benedict et al. 1999), to the catalogue from year 2010, and performed a new cross-match with the remaining sources in the 2015 catalogue (we used the PYTHON JPLEPHEM[2] software to calculate the parallax factors at each epoch). The values of PM and parallax used to shift the catalogues are available in Table 2.[3]

For the cross-match between the catalogues, we used a 0.35 arcsec tolerance radius and allowed a difference of up to 0.3 mag for the corresponding band, which is the photometric uncertainty in the *J* band at the 5σ detection limit. Given the high density of sources towards the galactic inner disc (∼900 000 objects deg^2 for the VVV limiting magnitude of *J* ∼ 19.5), after the cross-match we obtained nearly 50 sources per tile per band, per α Cen stellar member.

A match between these comoving candidates sources in the *Y* and *J* bands was performed, but not a single object was detected in the two bands, which was expected if there were no additional companions.

Nevertheless, we explore if there might be one real source detected in a single band. Most of the sources that passed the first cut were flagged as noise detections. So we decided to apply one more filter, selecting only sources that are flagged as stellar in the CASU catalogues (flag for stellar objects is −1), the last criterion rejected most sources around spikes of saturated stars, or near the edge of the detectors, and blended objects. The remaining candidates per tile, per band and per stellar member of the α Cen system now were reduced to five. We did a visual inspection of these sources in 1 × 1 arcmin^2 images, and searched for the source in the
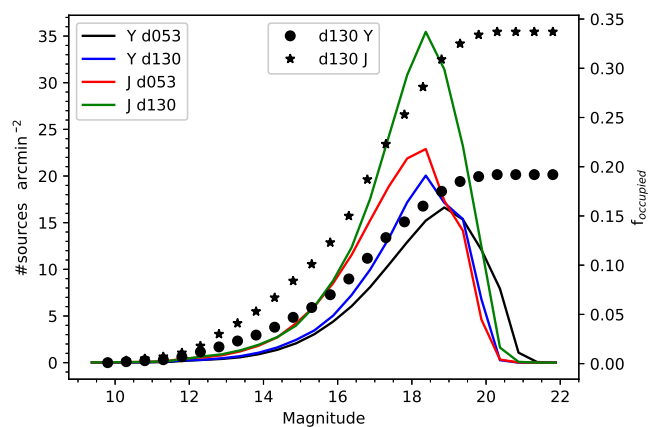
Figure 4. The density of sources per 0.5 mag bin per square arcminute for two tiles d130, the one with the largest number of sources, and d053, the tile that contains α Cen AB, both are the worst case scenarios in terms of highest source density and artefacts generated by the presence of an extremely bright source. Additionally, the right-hand side axis displays the cumulative area covered by stars brighter at any given magnitude (only tile d130 is shown); all the other tiles display a lower fraction of the image covered by stars.

original *Y*- and *J*-band images simultaneously.[4] We eliminated all these candidates, because in at least one of the bands we could see faint sources in both positions, but one of them not being detected by the finding/photometry routine, because of sensitivity or contrast issues caused by artefacts. For a handful of objects where we had doubts in both the *Y* and *J* bands, we looked at *Z*, *H* and *K*$_s$ band images, and we were able to confirm that there was a background source in each expected position. We did not find any source that passes all the matching criteria and the final visual inspection check.

We considered the possibility that at the epoch of observation a faint source might remain undetected because it was projected on the same position of a brighter background star. In Fig. 4, the number of sources per square arcmin per 0.5 mag bin is plotted, and also the cumulative fraction of the pixels on the image occupied by sources brighter at each given magnitude. We show here only the information for tiles d053 and d130, which are the worst case scenario, containing α Cen AB and the highest number of sources in the *J* band, respectively. It can be seen that below *J*, *Y* ∼ 16 mag there is less than 10 per cent chance of alignment, but it reaches to almost 30 per cent at the limiting magnitude in *J* band and 19 per cent at the *Y* band limit. Thus, the completeness of this search is at least 80 per cent, considering the results in the *Y* band. Nevertheless, all the fields were observed at different times in the *Y* and *J* bands, as explained above, which will decrease the effective area of occupied pixels and hence increase the completeness. Simply multiplying the covered fraction of the independent images would be the easiest way to calculate the final covering fraction, but most of the brightest sources will be detected over the same pixels, and introduce a strong correlation; therefore, the simple multiplication would be overoptimistic; we then adopt a conservative 85–88 per cent of completeness for the worst case scenario of tile d130, and ≳90 per cent for the remaining tiles.

---

[2] https://pypi.python.org/pypi/jplephem

[3] Repeating the process with the older values from *Hipparcos* astrometry from van Leeuwen (2007) and newer astrometry for Proxima from Lurie et al. (2014) does not give positive results either.

[4] On tile d129, we could use only *J* band because the *Y*-band image taken in 2010 was defective, producing twice the detections all over the field of view.
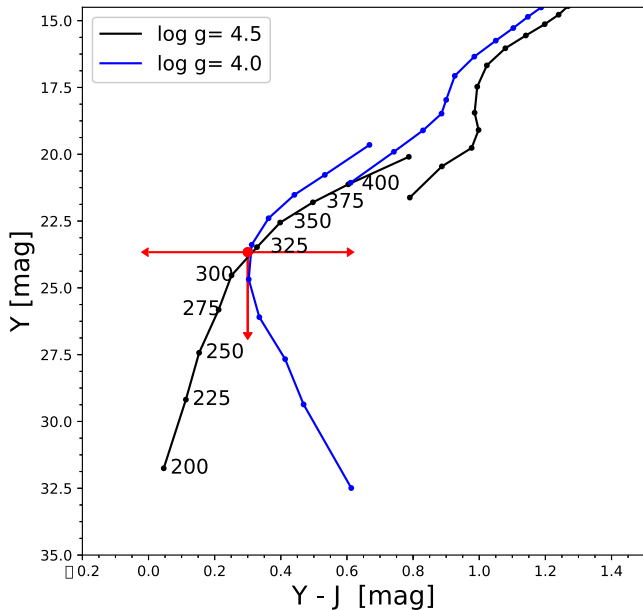
Figure 5. Colour and absolute magnitude from the atmospheric models from Morley et al. 2012 for T and Y dwarfs, and Morley et al. 2014 for Y dwarfs. For both models, we assumed a sedimentation factor of 5 and varied $\log(g)$ between 4 and 4.5. The 'jump' between the models at $T_{\rm eff} \sim 400$ K can be explained by the different cloud treatment in the two models. The red dot indicates the limiting magnitude in Y band and the colour given by the limits in Y and J bands.

4 DISCUSSION

For the α Cen system, there is a plethora of previous studies, and several properties are well constrained, a parallax of 747.17 ± 0.60 mas (1.338 ± 0.001 pc) (Kervella et al. 2016), a metallicity ([Fe/H] 0.23 ± 0.05 dex) (Ramírez, Allende Prieto & Lambert 2013) and an age between 4 and 7 Gyr (Eggenberger et al. 2004; Mamajek & Hillenbrand 2008; Boyajian et al. 2013; Bazot et al. 2016). The most stringent constraint on the presence of an extra companion in our study comes from the Y and J photometry. No source is detected up to a magnitude 19.3 and 19.0 mag in Y and J, respectively, within separations up to of 7000 au from α Cen AB system. The same photometric limits apply for Proxima, no companions to Proxima were found up to separations of 1200 au. To transform these magnitude limits to physical parameters, i.e. effective temperatures and masses, we used different atmospheric and evolutionary models.

First, we used the BD cloudy models from Morley et al. (2012) and Morley et al. (2014).[5] The first one reaches only up to $T_{\rm eff} = 400$ K and considers Na_2S, MnS, ZnS, Cr, KCl condensate clouds. The latter models assumes a 50 per cent cloud covered atmosphere, composed of H_2O ice in addition to the Na_2S, KCl, ZnS, MnS and Cra, These models reach $T_{\rm eff} = 200$ K. Based on these models, we were able to discard objects with $T_{\rm eff} > 325$ K for any given combination of sedimentation factor and surface gravity, these results can be seen in Fig 5, where we plot Y–J colour, against absolute Y magnitude.

Secondly, we tested with the atmospheric models of Saumon et al. (2012). These models include an improved line list of the NH_3 molecule, and of the collision-induced absorption of molecular hydrogen (H_2), no clouds opacities were considered for these

[5] The models from Morley et al. (2012, 2014) and Saumon et al. (2012) were taken from http://www.ucolick.org/cmorley/cmorley/Models.html.
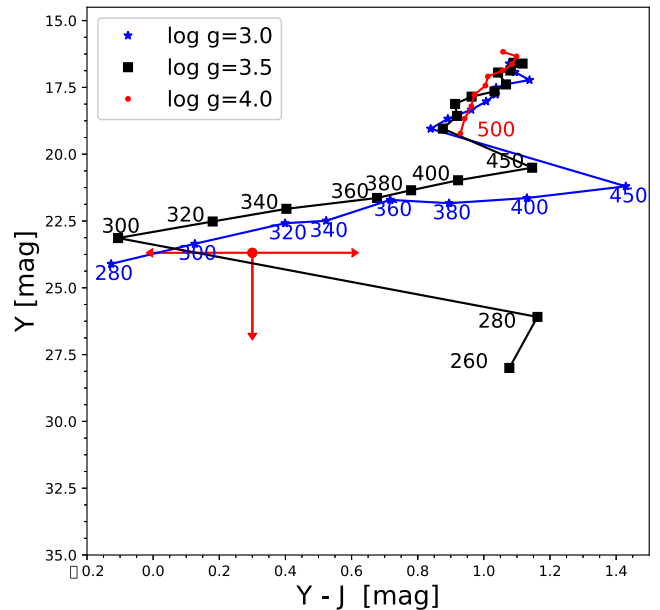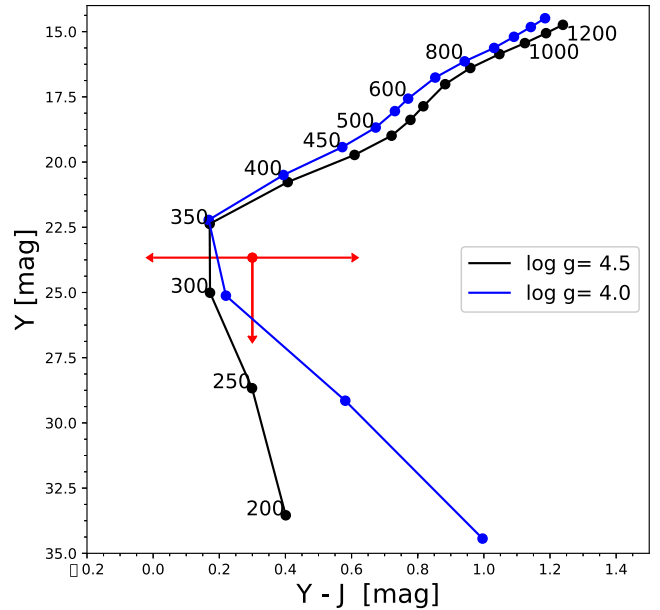

Figure 6. Colour and magnitude from the cloud-free atmospheric models upper panel: Saumon et al. (2012) for T and Y dwarfs. Assuming $\log(g)$ between 4 and 4.5. The red dot and arrows indicates our upper limit as in Fig. 5. Bottom panel: BT-Settl2011 models (Allard et al. 2012) for late T and Y dwarfs.

temperatures. The colours were calculated using the Saumon & Marley 2008 cloud-free evolution model grids. The limits for this model are shown in the upper panel of Fig. 6. Doing a simple linear interpolation of the data in the Y and J bands against effective temperature, considering values of $\log(g)$ between 4 and 4.5, and evaluating the limits obtained in Y and J bands (19.3 and 19.0 mag, respectively), we derived upper limits for the effective temperature of 326 and 322 K, for the Y and J bands, respectively.

Finally, we tested the BT-Settl models (Allard, Homeier & Freytag 2012),[6] which use the updated solar abundances from Caffau

[6] https://phoenix.ens-lyon.fr/Grids/BT-Settl/CIFIST2011/COLORS/

et al. (2011), and also account for a calibration of the mixing length based on radiation hydrodynamics simulations by Freytag et al. (2010) and adjustments to the MLT equations. To transform between the absolute magnitudes given at the surface of the BD provided by models, we assumed a radius of 0.1 $R_\odot$, which is that expected for these kinds of objects at ages around 4–7 Gyr (Burrows et al. 2001). Unfortunately, only objects with low surface gravities are available in the public grid of models at these low temperatures [log (g) 3.0 and 3.5], for higher gravities [log (g) 4.0 and 4.5] models are available for effective temperatures above 500 K. In the bottom panel of Fig. 6, it can be seen that the models with higher gravity and T_{eff} > 500 K are far above our limit, and indeed an extension of the models to higher gravities is required to compare the temperature limits with the other set of models. We also plot the lower gravity models to roughly estimate a limit in T_{eff}, and we can clearly see that objects with temperatures below 300 K are ruled out.

Assuming the distance from Kervella et al. (2016), and using the evolutionary models of Saumon & Marley (2008), with the atmosphere calculation described in Saumon & Marley (2008) and Marley et al. (2002). The cloudless model at the ∼320 K limit implies a mass of 10.5, 12.6 and 14.7M_{Jup}, for 4, 6 and 8 Gyr, and 9.4, 10.5 and 12.6M_{Jup}, for the cloudy model (with the cloud sedimentation factor 2), respectively. All these calculations were made assuming solar metallicity.

Our magnitude limits in *J* are the same as those of Mesa et al. (2017) for separations below 0.5 au. Here, we calculated a higher mass limit than Mesa et al. (2017) due to the use of an updated set of atmospheric models. If the same set of models is applied to their data set, the estimated limiting masses of the planets would increase by 2–3 M_{Jup}.

5 CONCLUSIONS

We have carried out a deep and wide search for other members of the α Cen system using the VVV NIR images. No additional companions were found around the α Cen AB system. In total, we explored a ∼19 sq. degree region around the α Cen AB system, ranging up to 7000 au to the south-east direction and nearly 20 000 au to the North-East and North-West direction. Also, no companions were found around Proxima within 1200 AU.

Our search considered a visual inspection in the K_s band and used photometric 5σ limits in the *Y*, *J* bands. The final limit excludes the presence of a BD/planet with a mass above 9.5–14.5 M_{Jup}, model- and age-dependent. Our search extended the limits on possible co-moving companions to the α Cen AB system and also Proxima to greater distances than previous attempts, complementing previous studies using radial velocities (Dumusque et al. 2012; Anglada-Escudé et al. 2016), higher spatial resolution imaging (Kervella et al. 2006; Mesa et al. 2017), deep optical imaging (Kervella & Thévenin 2007) and astrometric searches (Benedict et al. 1999).

An extended search will be possible in the following 2–3 yr making use of the on-going VVV extended survey (VVVX), which will extend the observed area by 2°.2 in the galactic latitude (positive and negative); this will allow us to place limits up to separations of ∼18 000 au in every direction.

ACKNOWLEDGEMENTS

REFERENCES

Allard F., Homeier D., Freytag B., 2012, R. Soc. Phil. Trans. Ser. A, 370, 2765
Anglada-Escudé G. et al., 2016, Nature, 536, 437
Astropy Collaboration et al., 2013, A&A, 558, A33
Baraffe I., Chabrier G., Barman T. S., Allard F., Hauschildt P. H., 2003, A&A, 402, 701
Bazot M., Christensen-Dalsgaard J., Gizon L., Benomar O., 2016, MNRAS, 460, 1254
Beamín J. C. et al., 2013, A&A, 557, LL8
Beamín J. C. et al., 2014, A&A, 570, L8
Beamín J. C. et al., 2015, MNRAS, 454, 4054
Beamin J. C. et al., 2017, Rev. Mex. Astron. Astrofis. Ser. Conf., 49, 159
Bendek E. A., Belikov R., Lozi J., Thomas S., Males J., Weston S., McElwain M., 2015, Proc. SPIE Conf. Ser. Vol. 9605, Space telescope design to directly image the habitable zone of Alpha Centauri. SPIE, Bellingham, p. 960516
Benedict G. F. et al., 1999, AJ, 118, 1086
Boyajian T. S. et al., 2013, ApJ, 771, 40
Burrows A., Hubbard W. B., Lunine J. I., Liebert J., 2001, Rev. Mod. Phys., 73, 719
Caffau E., Ludwig H.-G., Steffen M., Freytag B., Bonifacio P., 2011, Sol. Phys., 268, 255
Dalton G. B. et al., 2006, in Ian S. M., Masanori I., eds, Proc. SPIE Conf. Ser. Vol. 6269, The VISTA infrared camera. SPIE, Bellingham, p. 62690X
Dékány I., Minniti D., Catelan M., Zoccali M., Saito R. K., Hempel M., Gonzalez O. A., 2013, ApJ, 776, LL19
Demory B.-O. et al., 2015, MNRAS, 450, 2043
Dumusque X. et al., 2012, Nature, 491, 207
Eggenberger P., Charbonnel C., Talon S., Meynet G., Maeder A., Carrier F., Bourban G., 2004, A&A, 417, 235
Emerson J., Sutherland W., 2010, The Messenger, 139, 2
Endl M., Kürster M., 2008, A&A, 488, 1149
Freytag B., Allard F., Ludwig H.-G., Homeier D., Steffen M., 2010, A&A, 513, A19
Gonzalez O. A., Rejkuba M., Minniti D., Zoccali M., Valenti E., Saito R. K., 2011, A&A, 534, LL14
Hempel M. et al., 2014, The Messenger, 155, 29
Ivanov V. D. et al., 2013, A&A, 560, AA21
Ivanov V. D. et al., 2015, A&A, 574, A64
Kervella P., Thévenin F., 2007, A&A, 464, 373
Kervella P., Thévenin F., Coudé du Foresto V., Mignard F., 2006, A&A, 459, 669
Kervella P., Mignard F., Mérand A., Thévenin F., 2016, A&A, 594, A107
Kervella P., Thévenin F., Lovis C., 2017, A&A, 598, L7
Kurtev R. et al., 2017, MNRAS, 464, 1247
Leggett S. K., Tremblin P., Esplin T. L., Luhman K. L., Morley C. V., 2017, ApJ, 842, 118
Luhman K. L., Esplin T. L., 2016, AJ, 152, 78
Lurie J. C. et al., 2014, AJ, 148, 91
Mamajek E. E., Hillenbrand L. A., 2008, ApJ, 687, 1264-1293

Marley M. S., Seager S., Saumon D., Lodders K., Ackerman A. S., Freedman R. S., Fan X., 2002, ApJ, 568, 335

Mesa D. et al., 2017, MNRAS, 466, L118

Minniti D. et al., 2010, New A, 15, 433

Minniti D. et al., 2014, A&A, 571, AA91

Morley C. V., Fortney J. J., Marley M. S., Visscher C., Saumon D., Leggett S. K., 2012, ApJ, 756, 172

Morley C. V., Marley M. S., Fortney J. J., Lupu R., Saumon D., Greene T., Lodders K., 2014, ApJ, 787, 78

Pourbaix D., Boffin H. M. J., 2016, A&A, 586, A90

Quarles B., Lissauer J. J., 2016, AJ, 151, 111

Rajpaul V., Aigrain S., Roberts S., 2016, MNRAS, 456, L6

Ramírez I., Allende Prieto C., Lambert D. L., 2013, ApJ, 764, 78

Saito R. K. et al., 2012, A&A, 537, A107

Saumon D., Marley M. S., 2008, ApJ, 689, 1327

Saumon D., Marley M. S., Abel M., Frommhold L., Freedman R. S., 2012, ApJ, 750, 74

Schneider A. C., Cushing M. C., Kirkpatrick J. D., Gelino C. R., 2016, ApJ, 823, L35

Sirbu D., Thomas S., Belikov R., 2017, preprint (arXiv:1704.05441)

Smith L. C. et al., 2015, MNRAS, 454, 4476

Smith L. C., 2017, submitted

Taylor M. B., 2005, Astron. Data Anal. Softw. Syst. XIV. p. 29

Thomas S., Belikov R., Bendek E., 2015, ApJ, 810, 81

van Leeuwen F., 2007, A&A, 474, 653

Zapatero Osorio M. R. et al., 2016, A&A, 592, A80

APPENDIX A: INDIVIDUAL OBSERVATION DATES

We list here all the epochs used to obtain the magnitude limits in this study for the *Y* and *J* bands.

Table A1. VVV individual tile frames used in this study.

Tile name	Filter	Date
d013	*Y*	2010-03-27T03:25:15.8423
d013	*J*	2010-04-02T06:05:56.1283
d013	*Y*	2015-05-03T07:02:50.8657
d013	*J*	2015-06-08T05:23:57.1343
d014	*Y*	2010-03-27T03:38:32.1778
d014	*J*	2010-04-01T08:10:18.4379
d014	*Y*	2015-05-03T07:13:05.4679
d014	*J*	2015-06-08T05:50:55.0405
d015	*Y*	2010-03-28T05:07:37.9603
d015	*J*	2010-04-03T06:11:37.0379
d015	*Y*	2015-05-02T08:31:57.0208
d015	*J*	2015-05-04T07:29:17.1217
d016	*Y*	2010-03-29T03:54:26.5940
d016	*J*	2010-04-05T06:20:45.6914
d016	*Y*	2015-04-29T08:03:36.5387

Table A1 *– continued*

Tile name	Filter	Date
d016	*J*	2015-05-09T07:28:21.9441
d016	*J*	2015-05-14T06:57:05.1496
d052	*Y*	2010-03-27T03:52:31.8889
d052	*J*	2010-04-02T07:01:43.5797
d052	*Y*	2015-05-03T07:24:07.6892
d052	*J*	2015-06-08T06:16:15.7338
d053	*Y*	2010-03-28T05:23:19.5800
d053	*J*	2010-04-03T06:36:25.6897
d053	*Y*	2015-05-02T08:41:46.9336
d053	*J*	2015-05-04T07:53:33.6876
d054	*Y*	2010-03-28T05:36:12.4921
d054	*J*	2010-04-03T07:02:25.9449
d054	*Y*	2015-05-02T08:52:42.7697
d054	*J*	2015-05-04T08:24:04.8148
d090	*J*	2010-03-27T04:43:39.0487
d090	*Y*	2010-03-28T04:39:26.0940
d090	*Y*	2015-04-29T07:41:48.8063
d090	*J*	2015-05-09T04:52:36.3383
d091	*J*	2010-03-27T05:48:09.3985
d091	*Y*	2010-06-25T03:28:45.5742
d091	*Y*	2015-05-03T07:34:18.5241
d091	*J*	2015-05-29T04:31:46.7876
d091	*J*	2015-06-24T02:50:02.5166
d092	*J*	2010-03-29T05:16:06.8899
d092	*Y*	2010-06-16T04:52:10.5778
d092	*Y*	2015-04-16T09:08:36.6166
d092	*Y*	2015-04-16T09:18:28.5562
d092	*J*	2015-06-01T04:10:11.8593
d128	*J*	2010-03-27T05:08:24.3063
d128	*Y*	2010-03-28T04:54:23.8370
d128	*Y*	2015-04-29T07:52:16.4593
d128	*J*	2015-05-09T05:29:48.4227
d129	*J*	2010-03-27T06:10:27.3904
d129	*Y*	2010-06-25T03:45:04.0264
d129	*Y*	2015-05-03T07:46:03.7577
d129	*J*	2015-06-24T03:29:36.1733
d130	*J*	2010-03-27T06:32:28.5134
d130	*Y*	2010-06-25T03:59:50.6191
d130	*Y*	2015-05-03T07:56:15.7642
d130	*J*	2015-06-24T04:03:23.2328

This paper has been typeset from a T$_{\rm E}$X/L^{A}T$_{\rm E}$X file prepared by the author.